Anomalous vortex-ring velocities induced by thermally excited Kelvin waves and counterflow effects in superfluids

Giorgio Krstulovic and Marc Brachet

Laboratoire de Physique Statistique de l'Ecole Normale Supérieure, associé au CNRS et aux Universités Paris VI et VII, 24 Rue Lhomond, F-75231 Paris, France

(Received 15 February 2011; published 21 April 2011)

Dynamical counterflow effects on vortex evolution under the truncated Gross-Pitaevskii equation are investigated. Standard longitudinal mutual-friction effects are produced and a dilatation of vortex rings is obtained at large counterflows. A strong temperature-dependent anomalous slowdown of vortex rings is observed and attributed to the presence of thermally excited Kelvin waves. This generic effect of finite-temperature superfluids is estimated using energy equipartition and orders of magnitude are given for weakly interacting Bose-Einstein condensates and superfluid ^{4}He. The relevance of thermally excited Kelvin waves is discussed in the context of quantum turbulence.

DOI: 10.1103/PhysRevB.83.132506 PACS number(s): 67.25.dk, 47.37.+q, 67.25.dm

Quantum vortices present in superfluids interact with the normal fluid producing *mutual-friction* effects that must be phenomenologically introduced into Landau's two-fluid model.[1,2] For superfluid ^{4}He, there is no generally accepted theory of mutual friction that is valid over the entire temperature range.[3] For Bose-Einstein condensates (BECs), the Gross-Pitaevskii equation (GPE) is a dynamical description that was thought to be valid only in the low-temperature limit.[4] Davis *et al.*[5] suggested that, when a truncation of Fourier modes is performed, the resulting truncated GPE (TGPE) can also describe the (classical) thermodynamic equilibrium of a homogeneous BEC.[5] The TGPE was found to relax toward (microcanonical) equilibrium and a condensation transition was obtained.[5,6] Vortex dynamics was studied within the TGPE by Berloff and Youd,[7] who observed a dissipative contraction of vortex rings.

The purpose of this Brief Report is to investigate mutual friction and counterflow effects in the context of the TGPE. We present a stochastic algorithm that allows the efficient generation of grand canonical equilibrium states with nonzero momentum at given (target) values of temperature, chemical potential, and counterflow. These states are then combined with lattices of straight vortices and vortex rings, and their TGPE evolutions are monitored. Our main result is that, besides the phenomenologically expected counterflow effects, the TGPE also induces a (phenomenologically) unexpected slowdown of vortex rings that is caused by thermally excited Kelvin waves and should be considered in quantum turbulence.

The TGPE describing a homogeneous BEC of volume V is obtained from the GPE by truncating the Fourier transform of the wave function ψ: $\hat{\psi}_{\mathbf{k}} \equiv 0$ for $|\mathbf{k}| > k_{\max}$.[4,5] Introducing the Galerkin projector $\mathcal{P}_G$, which in Fourier space is $\mathcal{P}_G[\hat{\psi}_{\mathbf{k}}] = \theta(k_{\max} - |\mathbf{k}|)\hat{\psi}_{\mathbf{k}}$ with $\theta(\cdot)$ the Heaviside function, the TGPE explicitly reads

$$i\hbar\frac{\partial\psi}{\partial t} = \mathcal{P}_G\left[-\frac{\hbar^2}{2m}\nabla^2\psi + g\mathcal{P}_G[|\psi|^2]\psi\right], \qquad (1)$$

where $|\psi|^2$ is the number of condensed particles per unit volume, m is their mass, and $g = 4\pi\tilde{a}\hbar^2/m$, with $\tilde{a}$ the s-wave scattering length. The superfluid velocity reads $\mathbf{v}_s = (\hbar/m)\nabla\phi$, where ϕ is the phase of the (complex) ψ and h/m is the Onsager-Feynman quantum of velocity circulation around vortex lines $\psi = 0$.[4] When Eq. (1) is linearized around a constant $\psi = \hat{\psi}_{\mathbf{0}}$, the sound velocity is given by $c = (g|\hat{\psi}_{\mathbf{0}}|^2/m)^{1/2}$ with dispersive effects taking place for length scales smaller than the coherence length $\xi = (\hbar^2/2m|\hat{\psi}_{\mathbf{0}}|^2 g)^{1/2}$, which also corresponds to the vortex core size.

Equation (1) exactly conserves the energy $H = \int d^3x(\frac{\hbar^2}{2m}|\nabla\psi|^2 + \frac{g}{2}[\mathcal{P}_G|\psi|^2]^2)$ and the number of particles $N = \int d^3x|\psi|^2$. The momentum $\mathbf{P} = \frac{i\hbar}{2}\int d^3x(\psi\nabla\overline{\psi} - \overline{\psi}\nabla\psi)$ is also conserved when standard Fourier pseudospectral methods are used, provided that they are dealiased using the 2/3 rule ($k_{\max} = 2/3 \times M/2$, Ref. 8, at resolution M). [Global momentum conservation is mandatory to correctly describe vortex–normal-fluid interactions. When the nonlinear term in Eq. (1) is written, as in Ref. 5, $\mathcal{P}_G[|\psi|^2\psi]$, dealiasing must be performed at $k_{\max} = M/4$.]

Microcanonical equilibrium states are known to result from long-time integration of the TGPE.[5–7] Grand canonical states are given by the probability distribution $\mathbb{P}_{st}[\psi] = \mathcal{Z}^{-1}\exp[-\beta(H - \mu N - \mathbf{v}_n\cdot\mathbf{P})]$. They allow the direct control of temperature (instead of energy in a microcanonical framework). These states can be efficiently obtained by constructing a stochastic process that converges to a realization with probability $\mathbb{P}_{st}[\psi]$.[9] This process is defined by a Langevin equation consisting in a stochastic Ginbzurg-Landau equation (SGLE):

$$\hbar\frac{\partial\psi}{\partial t} = \mathcal{P}_G\left[\frac{\hbar^2}{2m}\nabla^2\psi - g\mathcal{P}_G[|\psi|^2]\psi\right] + \mathcal{P}_G\left[\mu\psi - i\hbar\mathbf{v}_n\cdot\nabla\psi\right] + \sqrt{\frac{2\hbar}{V\beta}}\mathcal{P}_G\left[\zeta(\mathbf{x},t)\right], \qquad (2)$$

where the white noise $\zeta(\mathbf{x},t)$ satisfies $\langle\zeta(\mathbf{x},t)\zeta^*(\mathbf{x}',t')\rangle = \delta(t-t')\delta(\mathbf{x}-\mathbf{x}')$, β is the inverse temperature, μ the chemical potential, and $\mathbf{v}_n$ the normal velocity. The term $i\hbar\mathbf{v}_n\cdot\nabla\psi$ induces an asymmetry in the repartition of sound waves and generates nonzero momentum states. These states do not generally correspond to a condensate moving at velocity $\mathbf{v}_s = \mathbf{v}_n$ because $\mathbf{v}_s$ is the gradient of a phase and takes

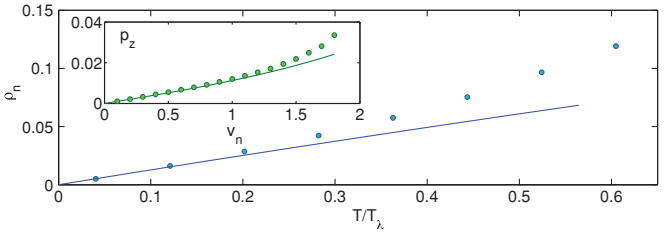

FIG. 1. (Color online) Temperature dependence of the normal density ρ_n (see text). Inset: P_z as a function of v_n at fixed temperature $T = 0.08T_\lambda$. Points, SGLE (2) equilibration at resolution 64^3; solid lines, low-temperature exact results.

discrete values for finite-sized systems. Equilibrium states with nonzero values of the counterflow $\mathbf{w} = \mathbf{v}_n - \mathbf{v}_s$ are generated in this way.

Using this algorithm in Ref. 9 the microcanonical and grand canonical ensembles were shown to be equivalent and the condensation transition reported in Refs. 5 and 6 identified with the standard second-order λ transition. All of the SGLE equilibria used in this Brief Report have a condensate at rest ($\mathbf{v}_s = \mathbf{0}$) and therefore $\mathbf{v}_n = \mathbf{w}$.

At low temperatures the partition function $\mathcal{Z}$ can be exactly computed by the steepest-descent method.[9] In particular, setting $\mathbf{v}_n = (0,0,v_n)$ the momentum of the equilibrium state reads $P_z = \frac{\mathcal{N}}{\beta}\frac{m}{\mu} f[\frac{4m\mu}{\hbar^2 k_{max}^2}]v_n$, where $\mathcal{N} = k_{max}^3 V/6\pi^2$ is the total number of modes and $f[z] = z - z^{3/2}\cot^{-1}(\sqrt{z})$. These relations furnish an explicit expression for the normal density $\rho_n = \frac{1}{V}\frac{\partial P_z}{\partial v_n}|_{v_n=0}$.

The direct control of the counterflow v_n in the SGLE algorithm allows the temperature dependence of ρ_n in the TGPE context to be obtained. The low-temperature exact results are in good agreement with SGLE data; see Fig. 1.

In all the numerical simulations presented in this Brief Report μ is adjusted in order to fix the density $\rho = mN/V$ to 1 and the physical constants in Eqs. (1) and (2) are determined by the relations $\xi k_{max} = 1.48$ and $c = 2$. The inverse temperature is normalized as $\beta = \mathcal{N}/VT$ and $V = (2\pi)^3$. With this choice of parametrization the λ-transition temperature is independent of $\mathcal{N}$ and its value is fixed to $T_\lambda = 2.48$; the quantum of circulation h/m has the value $c\,\xi/\sqrt{2}$.

We now turn to counterflow effects. To wit, we use an array of alternate-sign straight vortices $\psi_{lattice}$ (see Ref. 10). This exact stationary solution of the GPE is obtained by Newton's method. The vortices are separated by a distance π and can be considered isolated when $\xi \to 0$, as the resolution is increased. An equilibrium state ψ_{eq} is prepared using the SGLE (2) with counterflow v_n perpendicular to the vortices. The initial condition $\psi = \psi_{lattice} \times \psi_{eq}$ is then evolved with the TGPE. Figure 2(a) displays three-dimensional (3D) visualizations of the density at $t = 0$ and 100 where the displacement of the lattice is apparent. The temporal evolutions of the (parallel and perpendicular to $\mathbf{v}_n$) positions of a vortex $(R_\parallel, R_\perp)$ are presented in Fig. 2(c) for $T = 0.2\,T_\lambda$, $T = 0.4\,T_\lambda$, and $v_n = 0.4$. The counterflow-induced vortex velocity clearly depends on temperature. A perpendicular motion is also induced at short times. This motion has two phases: first an adaptation, making the lattice slightly imperfect, followed by a much slower perpendicular motion. Observe that the imperfection of the

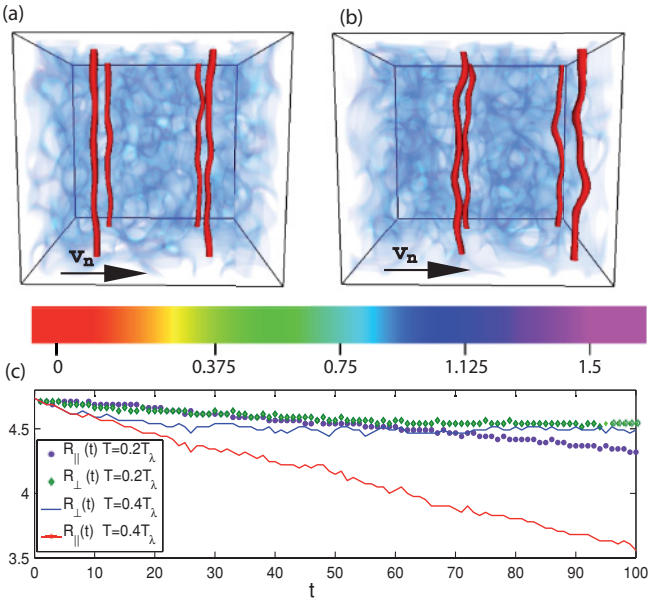

FIG. 2. (Color online) (a), (b) Density at $t = 0$, 100 of the lattice configuration (red lines) with $T = 0.4T_\lambda$ and $v_n = 0.4$. Blue clouds correspond to density fluctuations. (c) Positions $(R_\parallel, R_\perp)$ of a single vortex for $T = 0.2T_\lambda$, $T = 0.4T_\lambda$, and $v_n = 0.4$. Resolution 64^3.

lattice at final configurations is almost equal for the two temperatures presented in Fig. 2(c), but the parallel velocities are considerably different. The self-induced parallel velocity caused by the slight lattice imperfection is thus very small and does not drive the longitudinal motion.

We now concentrate on the measurement of $R_\parallel$ for which the present configuration is best suited. $R_\parallel$ has a linear behavior that allows direct measurement of the parallel velocity $v_\parallel$. The

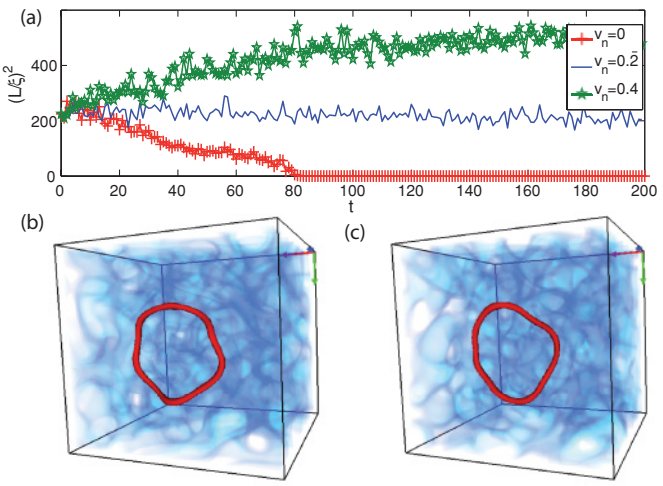

FIG. 3. (Color online) (a) Temporal evolution of the (squared) length of a vortex ring at different values of counterflow v_n (temperature $T = 0.4T_\lambda$ and initial radius $R = 15\xi$). (b), (c) 3D visualization of the vortex ring ($R = 20\xi$) and density fluctuations at $t = 18$, 19, with $T = 0.4T_\lambda$ and resolution 64^3. As in Fig. 2, the vortex rings are red loops and the blue clouds correspond to density fluctuations. Thermally excited Kelvin waves are apparent.

temperature dependence of $v_\parallel/v_n$ is presented in Fig. 3 for different values of v_n and ξ. This behavior is consistent with the standard phenomenological model for the vortex line velocity $\mathbf{v}_L$:[3]

$$\mathbf{v}_L = \mathbf{v}_{sl} + \alpha \mathbf{s}' \times (\mathbf{v}_n - \mathbf{v}_{sl}) - \alpha' \mathbf{s}' \times [\mathbf{s}' \times (\mathbf{v}_n - \mathbf{v}_{sl})], \quad (3)$$

where $\mathbf{s}'$ is the tangent of the vortex line, and $\mathbf{v}_{sl} = \mathbf{v}_s + \mathbf{u}_i$ is the local superfluid velocity with $\mathbf{u}_i$ the self-induced vortex velocity and $\mathbf{v}_n$ the normal velocity. The mutual-friction coefficients in Eq. (3) are typically written as $\alpha = B\rho_n/2\rho$, $\alpha' = B'\rho_n/2\rho$ where B and B' are of order 1 and weakly temperature dependent. Equation (3) applied to a straight vortex with v_n perpendicular to the vortex and $v_s = 0$ yields $\alpha' = v_\parallel/v_n$. The value of $\alpha' = B'\rho_n/2\rho$ with $B' = 0.83$ is displayed in Fig. 3 (bottom dashed line) and is in good agreement with the lattice data.

We now turn to the interaction of vortex rings and counterflow. The Biot-Savart self-induced velocity of a perfectly circular vortex ring of radius R is given by

$$u_i = \frac{\hbar}{2m}\frac{C(R/\xi)}{R}, \quad C(z) = \ln(8z) - a \quad (4)$$

where a is a core model-dependent constant.[3] We have checked, with initial data ψ_{ring} prepared using Newton's method, that the GPE (large-R/ξ) ring translational velocity is well reproduced by (4) with $a = 0.615$.

Equation (3) with v_n perpendicular to the ring and $v_s = 0$ yields the radial velocity $\dot{R} = -\alpha(u_i - v_n)$. The case without counterflow ($v_n = 0$) was studied by Berloff and Youd[7] and a contraction of vortex rings compatible with (3) was reported. To study the influence of counterflow we prepared an initial condition $\psi = \psi_{ring} \times \psi_{eq}$ in the same way as above for the vortex lattice. The temporal evolution of the (squared) vortex length of a ring of initial radius $R = 15\xi$ at temperature $T = 0.4T_\lambda$, and $v_n = 0$, 0.2, and 0.4 is displayed in Fig. 4(a). The Berloff-Youd contraction[7] is apparent in the absence of counterflow (bottom curve). The temperature dependence of the contraction, related to the α coefficient in Eq. (3), also quantitatively agrees with their published results (data not shown).

A dilatation of vortex rings is obtained [top curve in Fig. 4(a)] when the counterflow v_n is large enough. Such a

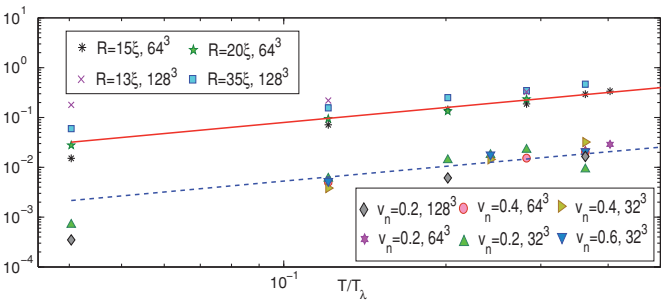

FIG. 4. (Color online) Temperature dependence of counterflow-induced lattice velocity $v_\parallel/v_n$ (bottom) and ring slowdown $\Delta v_L/u_i$ (top) obtained with $v_n = 0$. Dashed line, prediction of Eq. (3) with $\alpha' = 0.83\rho_n/2\rho$; solid line, prediction of anomalous slowdown by Eq. (6) with $R = 20\xi$ at various resolutions.

dilatation—a hallmark of counterflow effects—is expected[3] to correspond to a change of sign of $\mathbf{v}_n - \mathbf{v}_{sl}$ in Eq. (3). However, the predictions of Eq. (3) unexpectedly turn out to be quantitatively wrong. Indeed, using Eq. (4) with the conditions of Fig. 4(a) one finds $\mathbf{v}_{sl} = \mathbf{u}_i = 0.39$, which is significantly larger than the normal velocity $v_n = 0.2$ around which dilatation starts to take place [see middle curve in Fig. 4(a)]. The prediction using Eq. (3) for the longitudinal velocity $v_L = (1 - \alpha')u_i + \alpha' v_n$ is also unexpectedly wrong. Using the value of α' determined above for the vortex array, one finds $v_L \sim 0.98u_i$ and from Eq. (4) one finds for v_L the value 0.38, which is larger than the measured value $v_L = 0.23$.

This anomaly of the ring velocity v_L is also present in the absence of counterflow ($v_n = 0$) where Eq. (3) predicts that α' should be given by $\Delta v_L/u_i \equiv (u_i - v_L)/u_i$. The temperature dependence of $\Delta v_L/u_i$ is displayed in Fig. 3 (top curve). Observe that $\Delta v_L/u_i$ is one order of magnitude above the transverse mutual friction coefficient α' measured on the lattice.

We now relate the thermally induced anomaly to the velocity v_a induced on a vortex ring by a single Kelvin wave of (small) amplitude A and (large) wave number $N_K/2\pi R$ obtained in the Local Induction Approximation (LIA) LIA[11] and Biot-Savart[12] frameworks. The velocity v_a reads [see Eq. (26) of Ref. 11]

$$v_a = u_i\left(1 - A^2N_K^2/R^2 + 3A^2/4R^2\right) \quad (5)$$

where u_i is the (undisturbed) ring velocity (4).

The TGPE model naturally includes thermal fluctuations that excite Kelvin waves as apparent in Figs. 4(b) and 4(c). We assume that the slowing down effect of each individual Kelvin wave is additive and that the waves populate all the possible modes. Kelvin waves being bending oscillations of the quantized vortex lines, their wave number must satisfy $k \leqslant k_\xi = 2\pi/\xi$. The total number of thermally excited Kelvin waves is thus $\mathcal{N}_{Kelvin} \approx Rk_\xi$.

The amplitude term $A^2N_K^2/R^2$ in (5) can be obtained by simple equipartition arguments. The energy of a (perfect) ring is $E = \frac{2\pi^2\rho_s\hbar^2}{m^2}R[C(R/\xi) - 1]$, with ρ_s the superfluid density.[3] A Kelvin wave produces a variation of the ring length $\Delta L = \pi A^2N_K^2/R$. Its energy can thus be estimated as $\Delta E = \frac{dE}{dR}\frac{\Delta L}{2\pi}$. Assuming $\Delta E = \beta^{-1}$, this yields, at low temperatures where $\rho_s \approx \rho$, $A^2N_K^2/R^2 = m^2\beta^{-1}/\pi^2\rho\hbar^2RC(R/\xi)$. (This formula predicts a UV-convergent rms amplitude that is in good agreement with TGPE data, with values small enough to avoid self-reconnections of the ring.) Replacing A^2/R^2 in Eq. (5), the dominant effect is obtained by summing up to $\mathcal{N}_{Kelvin}$ and it finally becomes

$$\frac{\Delta v_L}{u_i} \equiv \frac{u_i - v_a}{u_i} \approx \frac{\beta^{-1}m^2}{\pi^2\rho\hbar^2C(R/\xi)}k_\xi. \quad (6)$$

The thermally induced anomalous slowdown (6) is in good agreement with the TGPE data displayed in Fig. 3.

Fluctuating Kelvin waves also cause the effective vortex core to be larger than the "bare" core size ξ. However, it is not possible to interpret (6) as produced by a renormalization of ξ in Eq. (4). Indeed the (dominant) contribution to the slowdown effect of a number of Kelvin waves is $\sum_i A_i^2N_i^2/R^2$ [see

Refs. 11 and 12, and Eq. (5)], whereas their contribution to the (rms) core size is proportional to $\sqrt{\sum_i A_i^2}$. Thus, two Kelvin waves of (very) different wave numbers and equal amplitudes contribute equally to the rms core size but (very) differently to the slowdown effect.

We now extend (6) in order to take into account quantum effects and estimate orders of magnitude in the physical case of a BEC and superfluid ^{4}He. The dispersion relation of Kelvin waves $\omega(k) = \frac{\hbar}{2m}k^2 C(R/\xi)$ (Ref. 11) implies [using the relation $\hbar\omega(k_{\rm eq}) = \beta^{-1} = k_{\rm B}T$] that Kelvin waves are not in equipartition for wave numbers $k > k_{\rm eq} = [2mk_{\rm B}T/\hbar^2 C(R/\xi)]^{1/2}$, as quantum effects are relevant in this range (as in blackbody radiation).

For a weakly interacting BEC with mean interatomic particle distance $\ell \sim |\hat{\psi}_{\mathbf{0}}|^{-2/3}$ satisfying $\tilde{a} \ll \ell \ll \xi$ the condensation temperature is $T_\lambda \sim \hbar^2/k_{\rm B}m\ell^2$. For $T > T^*$, where $T^*/T_\lambda \sim C(R/\xi)\,\ell^2/\xi^2 \ll 1$, it is straightforward to show that $k_{\rm eq} > k_\xi$ and therefore that (6) directly applies and reads $\Delta v_L/u_{\rm i} \sim (\ell/\xi)[T/T_\lambda C(R/\xi)]$. For $T < T^*$, k_ξ must be replaced by $k_{\rm eq}$ in formula (6) and the slowdown becomes $\Delta v_L/u_{\rm i} \sim [T/T_\lambda C(R/\xi)]^{3/2}$.

At zero temperature it is natural to suggest that the quantum fluctuations of the amplitudes of Kelvin waves produce an additional effect. This effect can be estimated by using $\Delta E = \hbar\omega(k)/2$. It is radius independent and of order $\Delta v_L/u_{\rm i} \sim (\ell/\xi)^3$ (see Ref. 9).

In a low-T physical BEC, with a quantum distribution of sound waves, $\rho_n/\rho \sim (T/T_\lambda)^4$,[1] the standard effects (3) are of order $(T/T_\lambda)^4$. Thus, the additional effect should dominate in this limit. In the case of superfluid ^{4}He the GPE description is only expected to give qualitative predictions.[3] Nevertheless, this additional effect should also be dominant at low temperatures.

Kelvin waves, excited by vortex reconnection, are also relevant in the context of quantum turbulence[13] where Eqs. (3) and (4) overestimate the speed of the perturbed rings. In a dilute gas of vortex rings, (6) increases the time between collisions and inhibits reconnection. Dense vortex tangles should be studied using the full TGPE.

In summary we obtained and measured standard counterflow mutual-friction effects within the TGPE. Our main result is that vortex rings are decelerated by thermal fluctuations of Kelvin waves and that these fluctuations, generic in finite-temperature superfluids, produce an experimentally testable effect that dominates the standard effects at low temperatures.

We acknowledge useful scientific discussions with C. Barenghi. The computations were carried out at IDRIS (CNRS) and visualizations used VAPOR.[14]

[1] L. D. Landau and L. M. Lifshitz, *Course of Theoretical Physics*, Vols. VI and IX (Butterworth-Heinemann, London, 1987).
[2] W. F. Vinen, Proc. R. Soc. London Ser. A **242**, 493 (1957).
[3] R. J. Donnelly, *Quantized Vortices in Helium II* (Cambridge University Press, Cambridge, 1991).
[4] N. P. Proukakis and B. Jackson, J. Phys. B **41**, 203002 (2008).
[5] M. J. Davis, S. A. Morgan, and K. Burnett, Phys. Rev. Lett. **87**, 160402 (2001).
[6] C. Connaughton, C. Josserand, A. Picozzi, Y. Pomeau, and S. Rica, Phys. Rev. Lett. **95**, 263901 (2005).
[7] N. G. Berloff and A. J. Youd, Phys. Rev. Lett. **99**, 145301 (2007).
[8] D. Gottlieb and S. A. Orszag, *Numerical Analysis of Spectral Methods* (SIAM, Philadelphia, 1977).
[9] G. Krstulovic, Ph.D. Thesis Univesité Paris VI (2010) [http://tel.archives-ouvertes.fr/tel-00505813/fr/]; G. Krstulovic and M. Brachet, e-print arXiv:1010.0116.
[10] C. Nore, M. E. Brachet, E. Cerda, and E. Tirapegui, Phys. Rev. Lett. **72**, 2593 (1994).
[11] L. Kiknadze and Y. Mamaladze, J. Low Temp. Phys. **126**, 321 (2002).
[12] C. F. Barenghi, R. Hanninen, and M. Tsubota, Phys. Rev. E **74**, 046303 (2006).
[13] W. F. Vinen, Philos. Trans. R. Soc. London Ser. A **366**, 2925 (2008).
[14] [http://www.vapor.ucar.edu].